Ultrasound Intima-Media Thickness and Diameter Measurements of the Common Carotid Artery in Patients with Renal Failure Disease

Christos Loizou, Eleni Anastasiou, Takis Kasparis, Theodoros Lazarou, Marios Pantziaris, Constandinos Pattichis

Ultrasound Intima-Media Thickness and Diameter Measurements of the Common Carotid Artery in Patients with Renal Failure Disease

Christos P. Loizou[1*], Eleni Anastasiou[2],Takis Kasparis[2], Theodoros Lazarou[3], Marios Pantziaris[4] and Constandinos S. Pattichis[5]

[1]Department of Computer Science, Intercollege, P. O. Box 51604, CY-3507, Limassol, Cyprus {panloicy@logosnet.cy.net} [2]Cyprus University of Technology, Departement of Electical, Computer Engineering and Informatics, Limassol, Cyprus {takis.kasparis@cut.ac.cy} [3]Nephrology Clinic, Limassol General Hospital, Limassol, Cyprus, {t.lazarou@cytanet.com.cy} [4]Cyprus Institute of Neurology and Genetics, Nicosia, Cyprus, {pantzari@cing.ac.cy} } [5]Departement of Computer Science, University of Cyprus, Nicosia, Cyprus {pattichi@ucy.ac.cy}

Abstract. Although the intima-media thickness (IMT) of the common carotid artery (CCA) is an established indicator of cardiovascular disease (CVD), its relationship with renal failure disease (RFD) is not yet established. In this study, we use an automated integrated segmentation system based on snakes, for segmenting the CCA, perform measurements of the IMT, and measure the CCA diameter (D). The study was performed on 20 longitudinal-section ultrasound images of healthy individuals and on 22 ultrasound images acquired from 11 RFD patients. A neurovascular expert manually delineated the IMT and the D in all RFD subjects. All images were intensity normalized and despeckled, the IMC and the D, were automatically segmented and measured We found increased IMT and D measurements for the RFD patients when compared to the normal subjects, but we found no statistical significant differences for the mean IMT and mean D measurements between the normal and the RFD patients.

Keywords: Intima-media thickness; carotid diameter; renal failure; ultrasound image; carotid artery.

1 Introduction

Cardiovascular disease (CVD), is the consequence of increased atherosclerosis, and is accepted as the leading cause of morbidity and mortality in patients with end-stage renal failure disease who undergo hemodialysis [1], [2]. Atherosclerosis, which is a buildup on the artery walls is the main reason leading to CVD and can result to heart attack, and stroke [1], [2]. Carotid intima-media-thickness (IMT) is a measurement of the thickness of the innermost two layers of the arterial wall and provides the distance between the lumen-intima and the media-adventitia. The IMT can be observed and measured as the double line pattern on both walls of the

longitudinal images of the common carotid artery (CCA) [2] (see also Fig. 1) and it is well accepted as a validated surrogate marker for atherosclerosis disease and endothelial dependent function [2].

Carotid IMT measurements have also been widely performed in hemodialysis patients with renal failure disease (RFD), and have shown that those patients have increased carotid IMT [3], impaired endothelium dependent, but unimpaired endothelium independent dilatation [4], compared to the age- and gender-matched normal controls. Furthermore, the traditional risk factors for increased atherosclerosis in the general population, such as dyslipidemia, diabetes mellitus, and hypertension, are also frequently found in RFD patients, and it was shown that those factors affect their vascular walls [5], [6]. Noninvasive B-mode ultrasound imaging is used to estimate the IMT of the human CCA [5]. IMT can be measured through segmentation of the intima media complex (IMC), which corresponds to the intima and media layers (see Fig. 1) of the arterial CCA wall. There are a number of techniques that have been proposed for the segmentation of the IMC in ultrasound images of the CCA, which are discussed in [7]. In two recent studies performed by our group [8], [9], we presented a semi-automatic method for IMC segmentation, based on despeckle filtering and snakes segmentation [10], [11]. In [9], we presented an extension of the system proposed in [8], where also the intima- and media-layers of the CCA could be segmented.

There have been a relatively small number of studies performed, for investigating the effect of increased IMT in the CCA and its relation to the progression of RFD. More specifically, in [12], carotid and brachial IMT were evaluated in diabetic and non-diabetic RFD patients undergoing hemodialysis. In [13], a correlation between the IMT and age in RFD patients was found, while in [14], kidney dysfunction was associated with carotid atherosclerosis in patients with mild or moderate chronic RFD. Increased IMT values in chronic RFD patients were also reported in [15], while in [16] it was shown that hemodialysis pediatric patients had reduced endothelial function with a development of carotid arteriopathy.

In this study, we use an automated integrated segmentation system based on snakes, for segmenting the CCA, perform measurements of the IMT and measure the CCA diameter (D). Our objective was to estimate differences for the IMT as well as for the D between RFD patients and normal subjects. Our study showed that the IMT and D are larger in ERD patients when compared with normal individuals. The study also showed that, there were no statistical significant differences for the IMT and the D measurements between the normal and the RFD patients. The findings of this study may be helpful in understanding the development of RFD and its correlation with atherosclerosis in hemodialysis patients.

The following section presents the materials and methods used in this study, whereas in section 3, we present our results. Sections 4 and 5 give the discussion, and the concluding remarks respectively.

2 Materials & Methods

2.1 Recording of ultrasound images

A total of 42 B-mode longitudinal ultrasound images of the CCA which display the vascular wall as a regular pattern (see Fig. 1a) that correlates with anatomical layers were recorded (task carried out by co-authors T. Lazarou and M. Pantziaris). The 20 images were from healthy individuals at a mean±SD age of 48±10.47 years and the 22 images were acquired from 11 RFD patients (1 woman and 10 men) at a mean±SD age of 55±12.25 years (5 patients had CVD symptoms). The images were acquired by the ATL HDI-5000 ultrasound scanner (Advanced Technology Laboratories, Seattle, USA) [17] with a resolution of 576X768 pixels with 256 gray levels. We use bicubic spline interpolation to resize all images to a standard pixel density of 16.66 pixels/mm (with a resulting pixel width of 0.06 mm). For the recordings, a linear probe (L74) at a recording frequency of 7MHz was used. Assuming a sound velocity propagation of 1550 m/s and 1 cycle per pulse, we thus have an effective spatial pulse width of 0.22 mm with an axial system resolution of 0.11 mm [17]. A written informed consent from each subject was obtained according to the instructions of the local ethics committee.

2.2 Ultrasound image normalization

Brightness adjustments of ultrasound images were carried out in this study based on the method introduced in [18], which improves image compatibility by reducing the variability introduced by different gain settings, different operators, different equipment, and facilitates ultrasound tissue comparability. Algebraic (linear) scaling of the images were manually performed by linearly adjusting the image so that the median gray level value of the blood was 0-5, and the median gray level of the adventitia (artery wall) was 180-190 [18]. The scale of the gray level of the images ranged from 0-255. Thus the brightness of all pixels in the image was readjusted according to the linear scale defined by selecting the two reference regions. Further details of the proposed normalization method can be found in [8]-[11].

2.3 Manual measurements

A neurovascular expert (task carried out by co-author M. Pantziaris) delineated manually (in a blinded manner, both with respect to identifying the subject and delineating the image by using the mouse) the IMC and the D [8], on all longitudinal ultrasound images of the CCA after image normalization (see subsection 2.2) and speckle reduction filtering (see subsection 2.4). The IMC was measured by selecting 20 to 40 consecutive points for the intima and the adventitia layers, while by selecting 30 to 60 consecutive points for the near and far wall of the CCA respectively. The manual delineations were performed using a system implemented in Matlab (Math Works, Natick, MA) from our group. The measurements were performed between 1 and 2 cm proximal to the bifurcation of the CCA on the far wall [18] over a distance

of 1.5 cm starting at a point 0.5 cm and ending at a point 2.0 cm proximal to the carotid bifurcation. The bifurcation of the CCA was used as a guide, and all measurements were made from that region. The IMT and the D were then calculated as the average of all the measurements. The measuring points and delineations were saved for comparison with the snake's segmentation method.

2.4 Speckle reduction filtering (DsFlsmv)

In this study the linear scaling filter (despeckle filter linear scaling mean variance-DsFlsmv) [19], utilizing the mean and the variance of a pixel neighborhood was used to filter the CCA ultrasound images from multiplicative noise prior the IMC and D segmentation. The filter may be described by a weighted average calculation using sub region statistics to estimate statistical measurements over 5x5 pixel windows applied for two iterations [10], [11]. Further implementation details of the DsFlsmv despeckle filter may be found in [10].

2.5 Automatic IMC and D snakes segmentation

The IMC and the D were automatically segmented after normalization and despeckle filtering (see section 2.2 and section 2.4), using an automated segmentation system proposed and evaluated in [8] and [9] based on a Matlab® software developed by our group. We present in Fig. 1b the automated results of the final snake contours after snakes deformation for the IMT at the far wall and the D, which were automatically segmented by the proposed segmentation system. An IMT and D initialization procedure was carried out for positioning the initial snake contour as close as possible to the area of interest, which is described in [8]-[10].

The Williams & Shah snake segmentation method [20] was used to deform the snake and segment the IMC and D borders. The method was proposed and evaluated in [8] and [9] for the IMC segmentation, in 100 ultrasound images of the CCA and more details about the model can be found there. For the Williams & Shah snake, the strength, tension and stiffness parameters were equal to $\alpha = 0.6$, $\beta_s = 0.4$, and $\gamma_s = 2$ respectively. The extracted final snake contours (see Fig. 1b), corresponds to the adventitia and intima borders of the IMC and the D at the near wall. The distance is computed between the two boundaries (at the far wall), at all points along the arterial wall segment of interest moving perpendicularly between pixel pairs, and then averaged to obtain the mean IMT (IMT_{mean}). The near wall of the lumen was also segmented for calculating the mean lumen of D (D_{mean}). Also the maximum (IMT_{max}, D_{max}), minimum (IMT_{min}, D_{min}), and median (IMT_{median}, D_{median}) IMT and D values,

were calculated. Figure 1b shows the detected IMT_{mean}, and D_{mean} on an ultrasound image of the CCA.

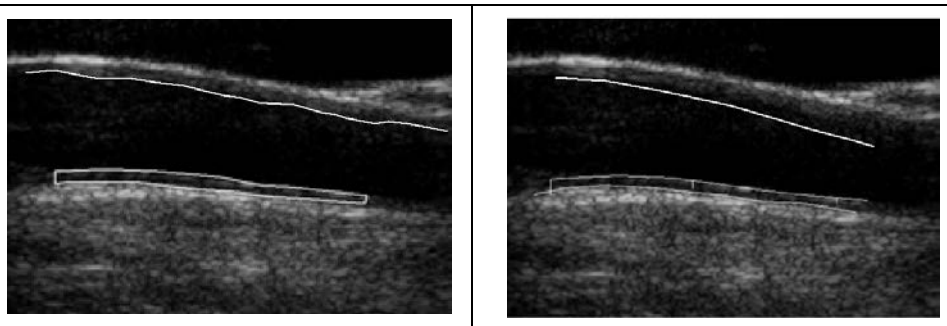

(a) Manual CCA IMT and D segmentations | (b) Automated CCA IMT and D segmentations

Figure 1. a) Manual IMC and D segmentation measurements (IMT_{mean}=0.73 mm, IMT_{max}=0.85 mm, IMT_{min}=0.55 mm, IMT_{median}=0.66 mm, D_{mean}=5.81 mm, D_{max}=5.95 mm, D_{min}=4.61 mm, D_{median}=5.73 mm), and b) automated IMC and D segmentation measurements (IMT_{mean}=0.72 mm, IMT_{max}=0.83 mm, IMT_{min}=0.51 mm, IMT_{median}=0.67 mm, D_{mean}=5.71 mm, D_{max}=5.75 mm, D_{min}=4.69 mm, D_{median}=5.75 mm) from an RFD patient at the age of 54.

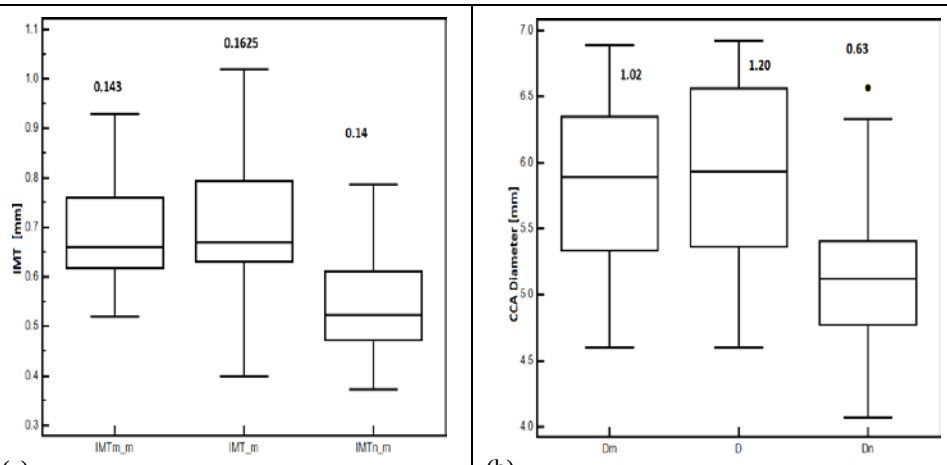

(a) (b)

Figure 2. Box plots for the mean values of the CCA for: (a) IMT, and (b) D. From left to right, mean manual IMT and Diameter (IMTn_m, Dm), mean automated IMT and Diameter (IMT_m, D) on RFD patients and mean manual IMT and diameter on normal subjects (IMTn_m, Dn) respectively. Inter-quartile rage values are shown above the box plots. Straight lines connect the nearest observations with 1.5 of the inter-quartile range (IQR) of the lower and upper quartiles. Unfilled rectangles indicate possible outliers with values beyond the ends of the 1.5xIQR.

2.6 Statistical analysis

The Wilcoxon rank sum test was used in order to identify if for each set of normal and RFD patients measurements as well as for the manual and automated segmentation measurements, a significant difference (S) or not (NS) exists between the extracted IMC and D measurements, with a confidence level of 95%. For significant

differences, we require $p<0.05$. Furthermore, box plots for the different measurements, were plotted. Bland–Altman plots [21], with 95% confidence intervals, were also used to further evaluate the IMT measurement agreement between the normal subjects and RFD patients. Also, the correlation coefficient, ρ, between the normal and RFD IMT and D measurements, which reflects the extent of a linear relationship between two data sets.

3 Results

We have evaluated 20 ultrasound images of the CCA from healthy subjects at a mean±SD age of 48±10.47 years and 22 ultrasound images acquired from 11 RFD patients (1 woman and 10 men) at a mean±SD age of 55±12.25 years, out of which 5 had CVD symptoms.

Figure 1 illustrates the manual (see Fig.1a) and the automated (see Fig. 1b) IMC and D segmentation measurements performed on a normalized despeckled ultrasound image of the CCA of an RFD patient at the age of 54.

Table 1 presents the IMC and D, segmentation measurements for the mean, maximum, minimum, and median IMT and D values on all normalized despeckled images of the CCA investigated in this study. These were performed on all images acquired from normal subjects (IMTn, Dn), as well as on all images acquired from the RFD patients, manually by the neurovascular expert (IMTm: 0.69±0.11 mm, Dm: 5.81±0.65 mm) and automated by the segmentation system (IMT: 0.71±0.13 mm, D: 5.96±0.72 mm).

After performing the non-parametric Wilcoxon rank sum test, we found no statistical significant differences between the aforementioned IMT and D measurement groups. More specifically we found $p = 0.44$, $p = 0.87$, and $p = 0.66$, for the IMT between the IMTm vs IMT, IMTm vs IMTn and IMT vs IMTn) and $p = 0.78$, $p = 0.61$, and $p = 0.89$, for the D between the Dm vs D, Dm vs Dn and D vs Dn). We also found no statistical significant difference between the manual and the automated IMT measurements ($p = 0.11$) of the CCA.

The correlation coefficient ρ, between the RFD manual and the automated IMT and D measurements (- / -) was ρ=0.30 / ρ=0.22 ($p = 0.15$ / $p = 0.91$), between the RFD manual and normal subjects IMT measurements was ρ=0.67 / ρ=0.56 ($p = 0.058$ / $p = 0.67$), and between the automated RFD and normal subjects IMT and D measurements was ρ=0.25 / ρ=0.46 ($p = 0.41$ / $p = 0.22$) respectively.

Figure 2a) presents box plots for the manual (IMTm_m) and the automated (IMT_m) mean IMT segmentation measurements for the RFD patients as well as for the automated IMT measurements (IMTn_m) from normal subjects. In Fig. 2b) we present box plots for the the CCA diameter measurements for the manual RFD patients (Dm), for the automated RFD patients (D), and for the manual segmentations (Dn) on the normal subjects. The IMT difference between the RFD automated and the normal subjects was (0.16±0.032) mm (see also Fig. 3). The difference between the manual and the automated IMT measurements for the RFD patients was (0.02±0.01) mm. Figure 3 illustrates a Bland–Altman plot between the automated mean IMT for all RFD patients (IMT_m) and the normal mean IMT (IMTn_m) segmentation

Table 1. Manual and Automated Mean, Maximum, Minimum And Median±(Standard Deviation) Measurements For The IMT And the D For 20 Normal and 22 RFD Patients. Values Are in mm. The Standard Deviations Are Given In Parentheses

	Mean (mm)	Maximum (mm)	Minimum (mm)	Median (mm)
CCA IMT				
IMT_n	0.55(0.10)	0.67(0.13)	0.41(0.09)	0.55(0.12)
IMT_m	0.69(0.11)	0.93(0.16)	0.57(0.17)	0.68(0.11)
IMT	0.71(0.13)	0.90(0.23)	0.53(0.23)	0.69(0.12)
CCA Diameter				
D_n	5.10(0.58)	5.23(0.61)	4.73(0.64)	5.12(0.56)
D_m	5.81(0.65)	5.99(0.62)	5.58(0.69)	5.66(0.62)
D	5.96(0.72)	6.08(0.68)	5.59(0.74)	5.78(0.71)

IMT_n, D_n: Automated IMT and D measurements from normal subjects. IMT_m, D_m, IMT, D: Manual and automated IMT and D measurements from RFD subjects.

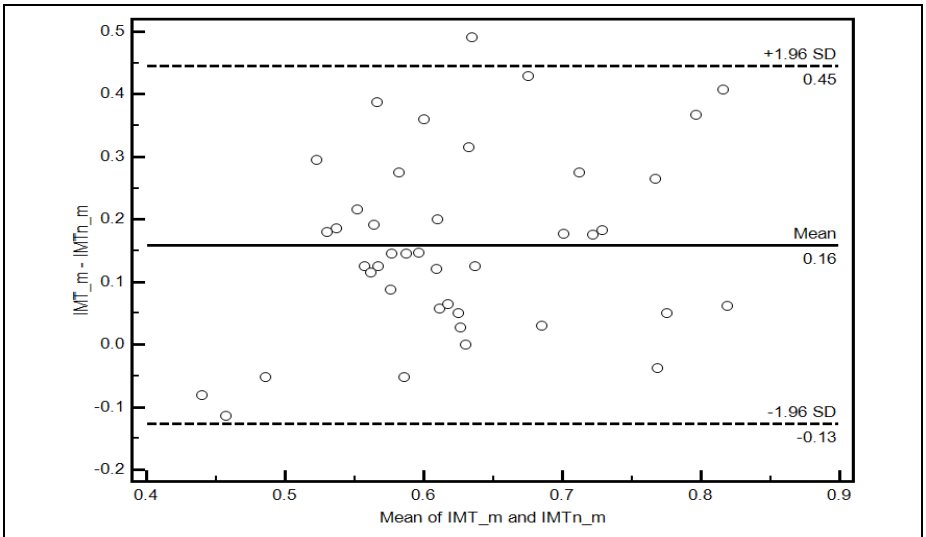

Figure 3. Regression lines (Bland–Altman plots) between the automated mean IMT for the RFD patients (IMT_m) versus the automated mean normal IMT (IMTn_m) of the CCA for all subjects. The middle line represents the mean difference, and the upper and lower two outside lines representthe limits of agreement between the two measurents, which are the mean of the data±2sd for the estimated difference between the two measurements.

measurements of the CCA for all subjects. As it is shown from Fig. 3, the difference of the two measurement methods was (0.16+0.45) mm and (0.16-0.13) mm.

4 Discussion

The results of this study showed that the IMT and D in the CCA of ERD patients are larger when compared with the values found for the normal subjects. The study also showed that, there are no statistical significant differences for the IMT and D measurements between the normal subjects and the RFD patients. We also found no statistical significant differences between the manual and the automated segmentation measurements for the IMC and the D. A difference was found between the automated segmented IMT mean (IMT_m) measurements of the RFD patients and the automated segmented mean IMT measurements of the normal subjects (IMTn_m) (see also Fig. 2a and Table 1). Although the aforementioned difference was estimated, we found no statistical significant differences for both the IMT and the carotid diameter, D, between those two measurements, as it was shown with the Wilcoxon rank sum test performed in this study. From Table 1, it is also obvious that the mean IMT and D for the normal subjects, exhibit both lower values when compared to the values of the RFD patients group. This is also the case for all other measurements of the IMT (mean, maximum, minimum, and median). Our findings show that kidney dysfunction may probably thus be associated with increased carotid IMT and carotid diameter, D. The subjects investigated in this study included a high proportion of patients with some atherosclerotic risk factors, indicating that kidney dysfunction is an atherosclerotic risk factor, especially in patients at high risk for CVD disease.

Atherosclerosis is the most common cause of RFD disease, resulting in hypertension and ischemic nephropathy [2], [5]. A regular follow up was suggested in [5], for selected patients with atherosclerotic renal artery stenosis before they develop severe hypertension or renal insufficiency. Randomized clinical trials will also be necessary to define the role of early renal revascularization in the management of these patients.

In a large study [22], where 1351 male individuals were investigated in order to estimate whether chronic RFD was associated with carotid IMT thickening, it was shown that chronic RFD may be associated with early carotid atherosclerosis in low-risk individuals, such as those undergoing general health screening, who have hypertension and/or impaired glucose metabolism.

In [12] the authors evaluated CCA IMT and brachial arteries, flow-mediated dilatation (FMD), and nitroglycerin-mediated dilatation (NMD) in diabetic and non-diabetic hemodialysis patients. In all patients a positive correlation was found with carotid and brachial IMT, and a negative one with FMD and NMD. With respect to hypertension as well as diabetes, a negative correlation was found with FMD and NMD. It was shown that age is the most important factor that significantly affected all studied markers of atherosclerosis in hemodialysis patients. According to their results, intensive antihypertensive treatment is recommended in hypertensive chronic hemodialysis patients. The authors in [13] found a correlation between IMT and age in RFD patients and that IMT values were correlated with total cholesterol. It was furthermore reported in [14], that kidney dysfunction was associated with increased carotid IMT independent of the classical atherosclerotic risk factors but they found no association between kidney dysfunction and calcified plaque. Carotid IMT may be a predictive marker of CVD disease that reflects early kidney dysfunction, especially in high-risk patients.

In another study [23], the relation between carotid IMT and hemodialysis patients in chronic RFD was investigated, where 78 RFD patients were examined. A significant positive correlation was found between IMT and hemodialysis ($p=0.045$) independent of traditional risk factors. It was also shown that hemodialysis patients had significantly higher mean IMT (1.136 ± 0.021 mm) compared to that of normal (0.959 ± 0.023 mm) patients. Similar findings were also reported in this study.

There are also some limitations for the present study which arises mostly from the small number of subjects included and that the duration of diabetes and RFD were not included. The material used in this study was acquired from RFD patients undergoing hemodialysis, where the 5 patients with CVD disorders were not studied separately. Additionally, the study should be further applied on a larger sample, a task which is currently undertaken by our group. Additional variables, such as age, sex, weight, blood pressure and others should be taken into account for better evaluating the RFD in hemodialysis patients.

5 Concluding Remarks

This paper presents a study on the carotid IMT and D measurements of the CCA in RFD patients undergoing haemodialysis. It was shown that the degree of atherosclerosis is greater in RFD patients when compared to that of normal subjects. We anticipate that the above comparison may have some clinical value in retrospectively screening of the dysfunction of the CCA through time. It would be furthermore interesting in the future to study the atherosclerotic carotid plaque changes in the aforementioned group of subjects and estimate whether and how kidney dysfunction is associated with the build-up of carotid plaques. It may also be possible to identify and differentiate those individuals into high and low risk groups according to their CVD risk before the development of plaques. The use of texture features will also be utilised in order to provide new feature sets, which can be used successfully for the classification of the IMC structures in normal and abnormal subjects. Future work will incorporate a new texture image retrieval system that uses texture features extracted from the IMC, to retrieve images that could be associated with the same level of the risk for developing RFD. Further research is required for estimating IMT and diameter differences between normal and RFD individuals in the CCA as well as their correlation with texture features extracted from these areas, and the progression of RFD.

References

1. Mendis, S., Puska, P., Norrving, B.: Global Atlas on cardiovascular disease prevention and control. WHO (2012) ISBN: 978-92-4-156437-3
2. Foley, R.N., Parfrey, P.S., Sarnak, M.J.: Clinical epidemiology of cardiovascular disease in chronic renal disease. Am. J. Kidney Dis. 32, 112--119 (1998)
3. Hojs, R.: Carotid intima-media thickness and plaques in hemodialysis patients. Artif. Organs 24, 691--695 (2000)

4. van Guldener, C., Lambert, J., Janssen, M.J., Donker, A.J., Stehouwer, C.D.: Endothelium-dependent vasodilatation and distensibility of large arteries in chronic hemodialysis patients. Nephrol. Dial. Transplant 12(Suppl. 2), 14--18 (1997)
5. Zielner, E.R.: Atherosclerotic renovascular disease: Natural history and diagnosis. Pers. Vasc. Surg. Endovasc. Ther. 16,4, 299--310 (2004)
6. Maeda, N., Sawayama, Y., Tatsukawa, M., et al.: Carotid artery lesions and atherosclerotic risk factors in Japanese hemodialysis patients. Atherosclerosis 169, 183--92 (2003)
7. Molinari, F., Zeng, G., Suri, J.S.: A state of the art review on intima-media thickness measurement and wall segmentation techniques for carotid ultrasound. Comp. Meth. and Progr. in Biomed. 100, 201--221 (2010)
8. Loizou, C.P., Pattichis, C.S, Pantziaris, M., Tyllis, T., Nicolaides, A.N.: Snakes based segmentation of the common carotid artery intima media. Med. Biolog. Eng. Comput. 45, 35--49 (2007)
9. Loizou, C.P., Pattichis, C.S., Nicolaides, A.N., Pantziaris, M.: Manual and automated media and intima thickness measurements of the common carotid artery. IEEE Trans. Ultras. Ferroel. Freq. Contr. 56, 5, 983--994 (2009)
10. Loizou, C.P., Pattichis, C.S.: Despeckle filtering algorithms and Software for Ultrasound Imaging. Synthesis Lectures on Algorithms and Software for Engineering, Ed. Morgan & Claypool Publishers, 1537 Fourth Street, Suite 228, San Rafael, CA 94901 USA (2008)
11. Loizou, C.P., Pattichis, C.S., Christodoulou, C.I., Istepanian, R.S.H., Pantziaris, M., Nicolaides A.: Comparative evaluation of despeckle filtering in ultrasound imaging of the carotid artery. IEEE Trans. Ultras. Ferroel. Freq. Contr. 52, 10, 1653--1669 (2005)
12. Rus, R., Butotovic-Ponikvar, J.: Intima media thickness and endothelial function in chronic hemodialysis patients. Therapeutic Apheresis and Dialysis 13, 4, 249--99 (2009)
13. Bevc, S., Hojs, R., Ekart, R., Hojs-Fabjan, T.: Atherosclerosis in hemodylaisis patienst: traditional and non-traditional risk factors. Acta Dermatoven, APA 15,4, 151--157 (2006)
14. Makiko, T., Abe, Y., Furukado, S., Miwa, K., et al.: Chronic kidney disease and carotid atherosclerosis. J. Stroke Cerebrov. Diseas. 21, 1, 47--51 (2012)
15. Somnath, D., Jayantha, P., Kanti, G.M., Kumar, A.D., et al.: Carotid artery intima-media thickness in chronic renal failure patients with diabetes and without diabetes. Int. J. Med. Scienc. 1, 3, 65--70 (2012)
16. Muscheites, J., Meyer, A.A., Drueckler E., et al.: Assessment of the cardiovascular system in pediatric chronic kidney disease: a pilot study. Pediatr. Nephrol. 23, 2233--2239 (2008)
17. A Philips Medical System Company, "Comparison of image clarity, SonoCT real-time compound imaging versus conventional 2D ultrasound imaging. ATL Ultrasound, Report (2001)
18. Elatrozy, T., Nicolaides, A.N., Tegos, T., Zarka, A., Griffin, M., Sabetai, M.: The effect of B-mode ultrasonic image standardization of the echodensity of symptomatic and asymptomatic carotid bifurcation plaque. Int. Angiol. 17, 3, 179--186 (1998)
19. Lee, J.S.: Refined filtering of image noise using local statistics. Comp. Graph. and Image Process. 15, 380--389 (1981)
20. Williams, D.J., Shah, M.: A fast algorithm for active contours and curvature estimation: Int. J. on Graph., Vision and Imag. Proc.: Image Underst. 55, 14--26 (1992)
21. Bland, J.M., Altman, D.G.: Statistical methods for assessing agreement between two methods of clinical measurement. Lancet 1, 8476, 307--310 (1986)
22. Ishizaka, N., Ishizaka, Y., Toda, E., Koike, K., et al.: Assosiation between chronic kidney disease and carotid intim-media thickness in individuals with hybertension and impaired glucose metabolism. Hypertens. Res. 30, 11, 1035--1041 (2007)
23. Paul, J., Dasgupta, S., Ghosh, K.M.: Carotid artery IMT as a surrogate marker of atherosclerosis in patients with chronic renal failure on hemodialysis. North Amer. J. Med. Sciens. 4, 2, 77--80 (2012)